

Dynamical Scaling: the Two-Dimensional XY Model Following a Quench

F. Rojas^{a,b*} and A. D. Rutenberg^c

^a*Department of Theoretical Physics, University of Manchester, Manchester, M13 9PL, UK*

^{b*}*Centro de Ciencias de la Materia Condensada, UNAM, Apartado Postal 2681, Ensenada, B.C., Mexico 22800*

^c*Centre for the Physics of Materials, Physics Department, McGill University, Montréal QC, Canada H3A 2T8*

(October 30, 2018)

To sensitively test scaling in the 2D XY model quenched from high-temperatures into the ordered phase, we study the difference between measured correlations and the (scaling) results of a Gaussian-closure approximation. We also directly compare various length-scales. All of our results are consistent with dynamical scaling and an asymptotic growth law $L \sim (t/\ln[t/t_0])^{1/2}$, though with a time-scale t_0 that depends on the length-scale in question. We then reconstruct correlations from the minimal-energy configuration consistent with the vortex positions, and find them significantly different from the “natural” correlations — though both scale with L . This indicates that both topological (vortex) and non-topological (“spin-wave”) contributions to correlations are relevant arbitrarily late after the quench. We also present a consistent definition of dynamical scaling applicable more generally, and emphasize how to generalize our approach to other quenched systems where dynamical scaling is in question. Our approach directly applies to planar liquid-crystal systems.

I. INTRODUCTION

The study of non-equilibrium dynamics in systems with continuous symmetries has burgeoned [1]. Liquid-crystalline systems [2–8], evolving after being quenched into an ordered phase, provide picturesque examples of topological defects and their interactions. Evolving systems of topological defects are also found in applications from cosmology [9] to quantum Hall ferromagnets [10,11].

A relatively simple system with a continuous symmetry is the two-dimensional XY ferromagnet with no disorder, which supports singular vortices that carry topological charge and have logarithmic interactions. The equilibrium properties have spawned a rich and fertile literature punctuated by the work of Kosterlitz and Thouless [12]. More recently, the non-equilibrium behavior of the 2D XY model following a quench to below the Kosterlitz-Thouless critical temperature, T_{KT} , has been studied theoretically [13–20] and also experimentally [3,5] with specially prepared liquid-crystal systems. Related 2D liquid-crystal systems have also been studied theoretically [21–23] and experimentally [2,4,8].

Following a quench at $t = 0$ from a disordered phase into an ordered phase, a crucial issue is whether there is dynamical scaling [24] at late times t , where

$$C(r, t) \equiv \langle \vec{\phi}(x, t) \cdot \vec{\phi}(x + r, t) \rangle = f(r/L). \quad (1)$$

Here, $\vec{\phi}$ is the XY order parameter, $f(x)$ is a time-independent scaling-function for the two-point correlations, and $L(t)$ is a growing length-scale that captures

all of the correlation dynamics. The explicit or implicit assumption of dynamical scaling underpins most theoretical descriptions of phase-ordering structure [1,25–27]. Unfortunately, apart from a limited number of solvable systems, there exist no theoretical approaches to *a priori* determine dynamical scaling. Indeed, the presence or absence of dynamical-scaling remains an unresolved issue in the 2D XY model [18,22]. This is surprising, since simple systems that break scaling are seen as exceptions [28]. For example, the weak scaling violations in the conserved spherical model identified by Coniglio and Zannetti [29] are due to non-commuting spherical and asymptotic-time limits [30] related to similar phenomena in equilibrium critical dynamics [31].

Stronger scaling violations are found in one- and two-dimensional systems with non-singular topological textures [11,32]. These systems segregate into domains of similarly charged textures, similar to the morphologies seen in reaction-diffusion $A + B \rightarrow \emptyset$ systems [33]. The domain-size and the texture separation provide distinct growing length-scales. Within this context, the difficulty in resolving scaling in the 2D XY model can be understood. Viewed as a plasma of overdamped charged vortices with logarithmic interactions [34], quenched from high-temperatures, the 2D XY model sits exactly at the marginal dimension ($d = 2$) below which segregated morphologies with strong scaling violations are expected, and above which a mixed morphology with only one length-scale, the particle separation, is seen [10]. Such *particle* systems are expected to scale, with no domain structure,

*Current and permanent address.

at the marginal dimension [10], however the asymptotic regime could be quite late.

With dissipative dynamics and the assumption of dynamical-scaling the predicted asymptotic growth-law of the characteristic length-scale is [27]

$$L(t) \simeq A(t/\ln[t/t_0])^{1/2}, \quad (2)$$

where A and t_0 are the non-universal amplitude and time-scale, respectively. This growth-law characterizes the correlations with a length $L_{1/2}(t)$, where $C(L_{1/2}, t) = 1/2$, as well as the vortex separation with a length-scale $L_v(t)$, where the vortex density $\rho_{def} = 1/L_v^2$. These lengths will only differ by prefactors and by subdominant contributions at late times. [Eqn. 2 also describes the annihilation time of an isolated vortex-antivortex pair with an initial separation L [17].] The logarithmic factor is crucial, and stems from the logarithmic vortex mobility. The same growth-law is expected in liquid-crystal films with vortices [27].

The analytical evidence for scaling violations is mostly suggestive: explicit violations in four-point correlations [16] and multiple energy-scales seen in energy-scaling calculations [27]. These would indicate multiple lengths which differ at most by logarithmic factors, consistent with the marginal dimensionality within a reaction-diffusion context [10]. Indeed, approximation schemes for correlation functions in the 2D XY model typically find scaling but with no logarithmic factors (see, e.g., [26,35], see also [36]). Additionally, the 2D XY model quenched *between* two temperatures below T_{KT} , and coarse-grained to a fixed scale to eliminate bound vortex pairs, is solvable [37] and dynamically scales without any logarithmic factor, $L(t) \sim t^{1/2}$.

Previous numerical evidence for scaling violations is stronger. Cell-dynamical simulations of XY models quenched to $T = 0$ by Blundell and Bray [18] found that two-point correlations did not scale well with respect to the defect separation L_v , though they scale with respect to the correlation length $L_{1/2}$ (see also [15,20]). Mondello and Goldenfeld [13] also found indications of multiple length-scales. Simulations of nematic films by Zapotocky *et al.* [22] found a variety of effective growth exponents, though again the correlation function appeared to scale (see also [21,23]). Other simulations on the 2D XY model at finite temperatures have recovered the expected growth law [17,19], and have found dynamical scaling [19]. Simulations of quenches to $T = 0$ in hard-spin systems found dynamical scaling of correlations even though the dynamics froze at late times [14]!

Experiments on liquid-crystal systems, following the pioneering work by Shiwaku *et al.* [2], have recovered the $t^{1/2}$ growth of defect separation after a quench, though with insufficient resolution to determine logarithmic factors [3–5,8] and with some difficulties in achieving an unbiased (symmetric) quench [4,5]. When measured, the structure [7,8] and other two-point correlations are consistent with dynamical scaling [3].

In this paper we want to clarify the existence or absence of dynamical scaling in the 2D XY model. A successful strategy can then be applied more generally to systems that seem to violate scaling, in particular to systems with more complicated collections of defects [28].

We first discuss the appropriate definition of dynamical scaling, within the context of systems relaxing after a quench. We then derive approximate forms for various correlation functions via Gaussian closure techniques, which impose scaling. While we do not expect them to exactly match the measured correlations, they are used to normalize the measured values in order to enhance our sensitivity to scaling or its absence. In combination with the growth-law, we have a “null hypothesis” which would be broken by scaling violations. We present our simulation data and find no evidence for scaling violations. We then explicitly reconstruct a two-point gradient correlation function, within the periodic system using only the vortex positions and charges, and find it significantly different from the unreconstructed scaling form. However both correlations scale with respect to the defect density. This indicates that both topological (vortex) and non-topological (“spin-wave”) contributions to the order parameter are asymptotically relevant, with characteristic lengths that remain asymptotically proportional.

II. DYNAMICAL SCALING

In phase-ordering, dynamical scaling colloquially means that there is a single characteristic length scale growing in time. This leads to a rough-and-ready symptom of dynamical scaling violations: multiple length-scales with distinct growth-laws, see for example [22,38]. While useful as a guide, this approach has limitations. One must first identify each asymptotic growth law, i.e. the effective exponent after it is constant in time and before finite-size effects of the sample become important. Practically, at most one or two decades in time are available in simulations if a 5% exponent variation is tolerated, and often less than a decade in experiments. When the scaling prediction for the growth-law is not *a priori* known, this approach on its own is dangerous. Indeed, sub-dominant corrections to the asymptotic growth law [39] can depend on the method used to extract the length-scale [40]. Even the observation of two asymptotically distinct length-scales does not demonstrate that they are dynamically interconnected. A silly example helps here: consider a sample made from gluing together a conserved binary-alloy system (asymptotic growth law $t^{1/3}$), and a non-conserved order-disorder alloy system (growth law $t^{1/2}$). Clearly two-growth laws could be observed in the hybrid, but they should not imply scaling violations. [Such dynamically independent sub-systems would lead to correlation functions that are sums of scaling functions.] The situation is more complicated when both lengths are observed within a homogeneous sample,

such as the asymptotic behavior of monopoles and vortex lines in bulk nematics [6]. Non-trivial inter-relationships of observed lengths can generally only be resolved with the help of simplified dynamical models, for example see [32,41].

A more precise definition of dynamical scaling is that two-point equal-time correlations have a time-independent scaling form, see Eqn. 1, which also implies scaling of the structure factor

$$S(k, t) \equiv \langle \vec{\phi}(k, t) \cdot \vec{\phi}(-k, t) \rangle = L^d g(kL), \quad (3)$$

where $g(x)$ is a time-independent scaling function. This is directly measured in scattering experiments, can be well approximated analytically, and is easy to extract from simulations. For systems with singular topological defects, such as domain walls, hedgehogs, vortices, or vortex lines, a generalized Porods law [1] connects the density of defect core ρ_{def} to the asymptotics of the structure via

$$S(k) \sim \rho_{def} k^{-(d+n)}, kL \gg 1, \quad (4)$$

where n characterizes the defect type [for the 2D XY model, $n = d = 2$]. This directly implies that the length derived from the defect density, L_v , is asymptotically proportional to the correlation length $L_{1/2}$ when the correlations dynamically scale.

This definition is still incomplete, since systems can satisfy Eqn. 3 yet have distinct lengths intimately connected by the dynamics — e.g. in the 1D XY model [32]. Additionally, higher-point correlations can be constructed in the 2D XY model which explicitly do *not* scale [16,42]. Should these be viewed as violations of dynamical scaling? Fortunately a self-contained definition of dynamical scaling exists, introduced by Bray and Rutenberg [27]. In order to calculate the rate of free-energy dissipation in a coarsening system, they additionally require the scaling of the time-derivative correlation function

$$T(r, t) \equiv \langle \partial_t \vec{\phi}(x, t) \cdot \partial_t \vec{\phi}(x + r, t) \rangle = (\dot{L}/L)^2 F(r/L) \quad (5)$$

where F is a new time-independent scaling function and $\dot{L} \equiv dL/dt$. Note that power-law growth, with or without additional logarithmic factors, implies that the prefactor $(\dot{L}/L)^2 \sim 1/t^2$. If dynamic scaling holds both for $T(r, t)$, as just defined, and for $C(r, t)$, then the growth exponent can be determined through a self-consistent energy-scaling approach [27,43]. This restricted definition of dynamical scaling, of both $C(r, t)$ and $T(r, t)$, picks up the scaling violations of the 1D XY model [32], and clearly separates the role of two-point from higher-point correlations [42]. We use this restricted definition here, and recommend it in the study of systems where dynamical scaling is questioned but Eqn. 1 seems to be satisfied.

III. DYNAMICS

We study purely dissipative quenches of 2D XY models from well above to below the Kosterlitz-Thouless transition temperature T_{KT} . Because of the line of critical points in the 2D XY model [12] the correlations in quenches to $0 < T < T_{KT}$ have a modified scaling form [19,37]. Essentially, critical equilibrium correlations have no characteristic length-scale and so the standard coarse-graining [1] to make temperature irrelevant to large-scale correlations is impossible. However, there is no indication that temperature changes dynamical scaling, or its absence, in the 2D XY model. Accordingly, in this paper, we only investigate quenches to $T = 0$. The non-conserved coarse-grained dynamics [44] are

$$\begin{aligned} F[\vec{\phi}] &= \int d^2x \left[(\nabla \vec{\phi})^2 + V_0(\vec{\phi}^2 - 1)^2 \right], \\ \partial_t \vec{\phi} &= -\Gamma \delta F / \delta \vec{\phi}, \\ \langle \vec{\phi}(\mathbf{x}, 0) \cdot \vec{\phi}(\mathbf{x}', 0) \rangle &= \Delta \delta(\mathbf{x} - \mathbf{x}'), \end{aligned} \quad (6)$$

where Γ is a kinetic coefficient that sets the time-scale, V_0 is the potential strength that sets the ‘hardness’ of the vector spins, and Δ characterizes the initial disordered state. The orientation of the two-component order parameter $\vec{\phi}(\mathbf{x})$ defines an angle $\theta(\mathbf{x}) \in [0, 2\pi]$, which is identical to the XY phase. The numerical implementation of the dynamics is discussed below in Sec. IV A.

In overview of the evolution: we start with a random high-temperature configuration and quench to $T = 0$. The order parameter locally equilibrates, but competition between degenerate ground-states leads to topologically stable vortices, with integer charges. The annihilation of oppositely charged vortices drives the subsequent dynamics, and characterizes one possible growing length scale — the vortex separation L_v . Of course, the order-parameter field around a moving vortex is not rigidly co-moving [27], and so non-singular “spin-wave” distortions are generated by the dynamics even at $T = 0$. The dynamics, emphasizing the vortices, can be visualized with a Schlieren pattern, see Fig. 1, analogous to those used in the study of liquid-crystal films [45].

A. Scaling Correlations from Gaussian Closure

Several approximation schemes eliminate high-order correlations in the evolution equation for two-point correlations [1,25,26,35,46]. We use a Gaussian-closure approximation, which gives quite good two-point correlations. We will use the results to normalize our correlations. This allows for a more sensitive test of scaling properties than has been possible before, and also highlights weaknesses of this approach (see also [15,47]).

For general $O(n)$ fields, we start with the Bray-Humayun-Toyoki (BPT) approach [35]. We introduce an auxiliary field \vec{m} parallel to the order parameter, $\vec{m} = \hat{\phi}$.

The zeros of \vec{m} match the positions of the topological defect cores, while $|\vec{m}|$ is roughly the distance to the closest defect core. Assuming a Gaussian probability distribution for \vec{m} results in two-point correlations between (r_1, t_1) and (r_2, t_2) :

$$C_g(r, t_1, t_2) = \frac{n\gamma}{2\pi} \left[B\left(\frac{1}{2}, \frac{n+1}{2}\right) \right]^2 F\left(\frac{1}{2}, \frac{1}{2}; \frac{n+2}{2}; \gamma^2\right), \quad (7)$$

where $r = |\mathbf{r}_2 - \mathbf{r}_1|$, $B(x, y)$ is the beta function, and $F(a, b, c; z)$ is the hyper-geometric function. The result is expressed in terms of the the normalized two-point, two-time correlation function of \vec{m} : $\gamma = \langle m(1)m(2) \rangle / [\langle m^2(1) \rangle \langle m^2(2) \rangle]^{1/2}$.

The various approximation schemes differ on the manner of determining γ . We use the the systematic approach introduced by Bray and Humayun [46] which produces

$$\gamma(r, t_1, t_2) = \left(\frac{4t_1 t_2}{(t_1 + t_2)^2} \right)^{d/4} \exp(-r^2/[4(t_1 + t_2)]), \quad (8)$$

where d is the spatial dimension. For equal-time correlations, we obtain the scaling form $C_g(r, t) = f_{BPT}(x)$, where $x = r/L$ and $L(t) = (4t)^{1/2}$. This highlights a problem with all existing correlation-closure approaches as applied to 2D XY models, since while they recover a scaling form they miss the logarithmic factor in the growth-law [36]. The same scaling variable is used in the time-derivative correlation function

$$T_g(r, t) = \frac{1}{16t^2} [\gamma^2 x^4 C_{\gamma\gamma}(x) + \gamma(x^4 - 4x^2 + 2d)C_\gamma(x)], \quad (9)$$

where $C_\gamma \equiv \partial C_g / \partial \gamma$ and $C_{\gamma\gamma} \equiv \partial^2 C_g / \partial \gamma^2$.

IV. SIMULATION

A. Simulation Methods

We use a standard CDS update [48] for soft spins, $\vec{\phi}(\mathbf{i}, t)$, on a periodic lattice, where t is now a discrete integer time and \mathbf{i} is the position:

$$\vec{\phi}(\mathbf{i}, t+1) = \frac{D}{4} \sum_{\mathbf{j}} \left[\vec{\phi}(\mathbf{j}, t) - \vec{\phi}(\mathbf{i}, t) \right] + E \hat{\phi}(\mathbf{i}, t) \tanh \left[\left| \vec{\phi}(\mathbf{i}, t) \right| \right], \quad (10)$$

where $\hat{\phi} = \vec{\phi} / |\vec{\phi}|$ is the unit vector. We use the standard values $D = 0.5$ and $E = 1.3$. The dynamics are stable and have the same attractors as Eqn. 6. We do not observe pinning effects in quenches to $T = 0$ (see

also [13,15,18,21,22]). The random initial conditions are chosen uniformly for each component from $[-0.1, 0.1]$.

We identify vortices with three methods that prove equally effective: by looking for the zeros in the vector field, by looking for plaquettes around which the phase rotates through $\pm 2\pi$, and by finding the peaks on the local energy density $E_{\mathbf{i}} = -\sum_{\mathbf{j}} \vec{\phi}(\mathbf{i}) \cdot \vec{\phi}(\mathbf{j})$, where the sum is over nearest neighbors of site \mathbf{i} . Due to the periodic boundary conditions, the system has no net vorticity.

In addition to tracking the number of vortices, we measure several correlations of the “hardened” order parameter, $\hat{\phi}(\mathbf{j}, t)$:

$$C(r, t) = \left\langle \hat{\phi}(\mathbf{j}, t) \cdot \hat{\phi}(\mathbf{j} + \mathbf{r}, t) \right\rangle. \quad (11)$$

The average $\langle \dots \rangle$ is over the independent sets of initial conditions, and includes a spherical average and an average over lattice sites \mathbf{j} . The structure factor is also calculated:

$$S(k, t) = \left\langle \vec{\phi}(-\mathbf{k}, t) \cdot \vec{\phi}(\mathbf{k}, t) \right\rangle. \quad (12)$$

We also measure the time derivative correlation function,

$$T(r, t) = \left\langle \delta_t \vec{\phi}(\mathbf{j}) \cdot \delta_t \vec{\phi}(\mathbf{j} + \mathbf{r}) \right\rangle, \quad (13)$$

where $\delta_t \vec{\phi} = \vec{\phi}(t+1) - \vec{\phi}(t)$ is a finite difference approximation for the time derivative.

To probe the distinction between vortex and non-vortex contributions to correlations, we measure a phase-gradient correlation function:

$$D(r, t) \equiv \langle \nabla \theta(\mathbf{j} + \mathbf{r}, t) \nabla \theta(\mathbf{j}, t) \rangle, \quad (14)$$

$$= h(r/L)/L^2, \quad (15)$$

where the second line is the natural scaling ansatz for the correlations. Note that $\langle \nabla \theta \rangle = 0$. We then reconstruct the vortex contribution $D_r(r, t)$ directly from the charges and locations of the vortices at a given time. From the vortex positions we build up the phase field $\nabla \hat{\theta}(\mathbf{j})$ using the periodic image of the minimal energy solution for each single vortex, $\nabla^2 \hat{\theta} = 0$, due to Grønbech-Jensen [49]:

$$d\theta/dx = -\pi \sum_{n=-\infty}^{\infty} \sin(2\pi y) / [\cosh(2\pi(x+n)) - \cos(2\pi y)],$$

$$d\theta/dy = \pi \sum_{n=-\infty}^{\infty} \sin(2\pi x) / [\cosh(2\pi(y+n)) - \cos(2\pi x)],$$

where x and y are the relative coordinates of the vortex in a system of size unity. The solutions for every vortex (with ± 1 factors for vortices and anti-vortices, respectively) were added together for every point in the system to obtain the fully-periodic *minimal-energy* phase-field consistent with the vortex configuration. [Direct reconstruction of the order-parameter field $\vec{\phi}$ proved intractable due various counter-charge effects imposed by

the periodic boundary conditions. In principle we could use our $\nabla\theta$ reconstruction to recover the order-parameter field with additional line-integrations.] To obtain more accurate vortex positions, we first identify the lattice plaquette by windings or energy peaks, then we use bilinear interpolation [50] to more accurately locate the zero of the order parameter within the plaquette. The sign of the vortex is determined by the winding of the phase field around the plaquette.

B. Simulation Results

We simulate a size 512×512 system, averaging over 40 independent samples. We check that there are no significant finite size effects in comparison to a 256×256 size system, with 20 samples. The data for reconstructed correlations is currently restricted to the 256×256 size system.

In Fig. 2 a), we plot $C(r,t)$ with respect to distance scaled by $L_{1/2}$ [$C(L_{1/2},t) = 1/2$]. The scaling is excellent, and the Gaussian-closure result (f_{BPT} , solid line) is indistinguishable from the data. In Fig. 2 b), however, the scaling collapse is not good with respect to the vortex separation [L_v , where $\rho = 1/L_v^2$] [18]. It is difficult to tell from this second plot alone whether scaling simply has a later onset time, or if scaling violations are indicated. This must be determined by a direct comparison of the length-scales L_v and $L_{1/2}$, as well as by a study of the time-derivative correlations $T(r,t)$, as discussed in Sec. II.

By normalizing the correlations with the Gaussian-closure result, C_g , we can sensitively probe scaling with the real-space correlations, see Fig. 3. While C_g is clearly too small at large scaled distance, correlations scale relatively well for $t \gtrsim 1000$.

The structure factor scales with respect to $L_k \equiv 1/\langle k \rangle$, its inverse first moment, see Fig. 4. Also shown (solid line) is the Fourier transform of the Gaussian-closure prediction, which slightly but systematically under and over-estimates the structure. By using a log-log plot we emphasize the $S(k) \sim \rho_{def} k^{-4}$ generalized Porod tail for $k/\langle k \rangle \gtrsim 2$, as per Eqn. 4. The good scaling of the Porod tail, which is determined by the vortex density, indicates that $L_k \sim L_v$ asymptotically.

We now directly test the assumption that all lengths asymptotically have the scaling growth-law of Eqn. 2 by plotting t/L^2 vs $\ln t$ for $L_{1/2}$, L_k , and L_v , in Fig. 5. The scaling prediction is a linear plot, with non-universal slope and intercept given by the amplitude A and time-scale t_0 . [Both of these can vary from one length-scale to another.] Linearity is observed for $\ln t \gtrsim 7.7$ ($t \gtrsim 2200$), in agreement with Fig. 3. We have fit them with straight lines with the same amplitude A but different t_0 . The correlation length $L_{1/2}$ has the strongest corrections to scaling, which is one cause of the bad scaling of $C(r,t)$ when plotted vs. L_v in Fig. 2 b). It is worth noting

that the growing length scales can also be well fit using effective exponents of 0.42, 0.40, and 0.40 (± 0.01), respectively, without logarithmic factors — see also [18,22]. However, if these effective exponents were asymptotically valid, and hence disagreed with the scaling prediction of Eqn. 2, we would not see scaling in the correlations [27].

While the two-point correlations $C(r,t)$ and $S(k,t)$ support dynamical scaling, we must also investigate the time-derivative correlation function, $T(r,t)$, as discussed in Sec. II. In Fig. 6, we scale lengths with respect to $L_{1/2}$, and remove the prefactor in Eqn. 5 by plotting $T(r,t)/T(L_{1/2},t)$. While scaling only sets in for $t \gtrsim 2000$, it is supported by the data. This correlation function has much more structure than the equal time correlations, such as a local maximum at $x \approx 2.3$ and a logarithmic divergence at small- x due to fast vortex annihilations. As a result, it provides a more stringent test of the Gaussian-closure approximation. We find significant discrepancies, the first to be found in two-point correlation functions.

Further confirmation of scaling in $T(r,t)$ is found by exploring the time dependence of the amplitude $T(L_{1/2},t) \sim t^{-\mu}$, see Fig. 7. The scaling form in Eqn.5 gives $\mu = 2$ (independent of logarithms), and we find $\mu = 2.0 \pm 0.1$. This is consistent with scaling. In combination with the scaling of $C(r,t)$ [and $S(k,t)$], and the consistency of the growth laws of *all* measured length scales with the scaling result, we conclude that the quenched 2D XY model dynamically scales.

In the equilibrium 2D XY model, the singular (vortex) and non-singular (spin-wave) degrees of freedom have independent contributions to the free energy [51]. Could it be possible for such distinct ‘singular’ and ‘non-singular’ length-scales to exist in phase-ordering systems (see, e.g., [52])? If separation of vortices and spin-waves occurs, we expect spin-wave contributions to have a characteristic scale $L \sim t^{1/2}$, i.e. to have a faster decay with no logarithmic factor [27]. In which case, the direct correlations should either have scaling violations due to the different length scale or the spin-waves should be asymptotically irrelevant — leaving the direct and reconstructed correlations asymptotically equal at late times. As can be seen from the snapshots of $|\nabla\theta|$ in Fig. 8, the reconstruction maintains the vortex locations and is periodic. Indeed, the reconstruction provides the *minimal energy* configuration consistent with vortex positions — in other words any ‘non-singular’ contribution is absent. In Fig. 9, the correlation function for the direct and reconstructed fields are shown as a function of the scaled distance. We first notice that both correlations scale with respect to $L_v = \rho^{-1/2}$ but with different functional forms. D_r has a sharper knee at $r\rho^{1/2} \simeq 0.7$, for example. This knee reflects the faster decay of $\nabla\theta$ from the vortex core in the reconstructed configurations, as is apparent in Fig. 8. The significant differences between the bare and reconstructed correlations in the scaling limit indicate that both vortex and “spin-wave” contributions are relevant to the direct correlations, and that the separation seen

in static properties does not hold in the dynamics.

The Porod plot of the Fourier-transformed correlations, see Fig. 10, further highlights the differences (note the $k \rightarrow 0^+$ intercepts). It is interesting that while $\langle \nabla \theta \rangle = 0$, the scaling curve has a non-conserved character. This is similar to correlations in globally-conserved systems. We also observe a k^{-2} Porod tail for $k/\rho^{1/2} \gtrsim 2$, which is expected from Fourier transforming the real-space scaling ansatz, Eqn. 15, and setting the amplitude of the Porod tail proportional to the vortex density $1/L^2$. The Porod tail has the same amplitude between the direct and reconstructed correlations, reflecting the singular structure of the vortex cores.

V. SUMMARY AND DISCUSSION

We find *no evidence for scaling violations* in the 2D XY model. All lengths, $L_{1/2}$, L_v , and L_k , have the same asymptotic form given by Eqn. 2, albeit with different non-universal coefficients. Real-space correlations, structure, and time-derivative correlations all scale as expected. Phase-gradient correlations, reconstructed from the vortex locations to have minimal energy and hence no spin-wave contributions, differed significantly from the direct correlations, indicating that both vortex and non-singular “spin-wave” contributions are asymptotically relevant. We expect similar results to hold in closely related planar liquid-crystal systems.

We have also shown how Gaussian-closure approximations can be useful to sensitively explore scaling. This has the added benefit of testing the approximation schemes. In particular we find significant discrepancies with respect to the measured time-derivative correlations, $T(r, t)$. More generally, we emphasize the role of sensitive null-like tests in checking apparent scaling violations. For example we plot the length-scales vs the expected growth law so that linear behavior is expected if scaling is obeyed. When scaling predictions are available, and in the face of transient corrections to scaling, this is preferable to the measurement of effective exponents.

One can never absolutely rule out scaling violations, if only because simulations and experiments can never reach $t \rightarrow \infty$. Each length in a system that dynamically scales will generically have different corrections to scaling. In quenches of the 2D XY model the leading correction is described well by t_0 , the time-scale of the logarithmic factor. Since scaling violations seem to be rare in quenched systems, the assumption should be that systems dynamically scale without strong evidence to the contrary — including the inability to perform a scaling collapse with *any* length-scale for either $C(r, t)$ or $T(r, t)$. This provides a self-consistent confirmation of dynamical scaling, provided the lengths used for the collapse are consistent with the same asymptotic growth-law. For some systems, including this one, the scaling growth-law can be independently determined. This is invaluable

when long-lived (logarithmically decaying) corrections to scaling are expected. The scaling of some other lengths in the problem can sometimes also be required for consistency. In this case the defect-separation scale L_v is needed to set the Porod amplitude, and hence must be consistent with the lengths L_k and $L_{1/2}$ extracted from $S(k, t)$ and $C(r, t)$, respectively.

VI. ACKNOWLEDGMENTS

F. Rojas thanks CONACYT (Mexico) and EPSRC (UK) grant GR/J24782, while A. D. Rutenberg thanks the NSERC, and *le Fonds pour la Formation de Chercheurs et l'Aide à la Recherche du Québec*. We would like to thank Alan Bray, Rob Wickham, and Martin Zapotocky for useful discussions.

-
- [1] A. J. Bray, *Adv. Phys.* **43**, 357 (1994).
 - [2] T. Shiwaku, A. Nakai, H. Hasegawa, and T. Hashimoto, *Polymer Comm.* **28**, 174 (1987).
 - [3] T. Nagaya, H. Hotta, H. Orihara, and Y. Ishibashi, *J. Phys. Soc. Jpn.* **61**, 3511 (1992); T. Nagaya, H. Orihara and Y. Ishibashi, *J. Phys. Soc. Jpn.* **64**, 78 (1995).
 - [4] A. N. Pargellis, P. Finn, J. W. Goodby, P. Panizza, B. Yurke, and P. E. Cladis, *Phys. Rev. A* **46**, 7765 (1992).
 - [5] A. N. Pargellis, S. Green, and B. Yurke, *Phys. Rev. E* **49**, 4250 (1994).
 - [6] B. Yurke, A. N. Pargellis, I. Chuang, and N. Turok, *Physica B* **178**, 56 (1992).
 - [7] A. P. Y. Wong, P. Wiltzius, and B. Yurke, *Phys. Rev. Lett.* **68**, 3583 (1992).
 - [8] A. P. Y. Wong, P. Wiltzius, R. G. Larson, and B. Yurke, *Phys. Rev. E* **47**, 2683 (1993).
 - [9] See, e.g., U.-L. Pen, U. Seljak, and N. Turok, *Phys. Rev. Lett.* **79**, 1611 (1997). See also *Formation and Interactions of Topological Defects* NATO ASI B349, edited by A.-C. Davis and R. Brandenberger, (Plenum, New York, 1995).
 - [10] A. D. Rutenberg, *Phys. Rev. E* **58**, 2918 (1998).
 - [11] A. D. Rutenberg, W. J. Zakrzewski, and M. Zapotocky, *Europhys. Lett.* **39**, 49 (1997).
 - [12] J. M. Kosterlitz and D. J. Thouless, *J. Phys. C* **6**, 1181 (1973).
 - [13] M. Mondello and N. Goldenfeld, *Phys. Rev. A* **42**, 5865 (1990).
 - [14] A. J. Bray and K. Humayun, *J. Phys. A* **23**, 5897 (1990).
 - [15] R. E. Blundell and A. J. Bray and S. Sattler, *Phys. Rev. E*, **48**, 2476 (1993).
 - [16] A. J. Bray, *Phys. Rev. E* **47**, 228 (1993).
 - [17] B. Yurke, A. N. Pargellis, T. Kovacs, and D. A. Huse, *Phys. Rev. E* **47**, 1525 (1993).
 - [18] R. E. Blundell and A. J. Bray, *Phys. Rev. E* **49**, 4925 (1994);

- [19] J. Rim Lee, S. J. Lee and B. Kim, Phys. Rev. E **52**, 1550 (1995).
- [20] H. Toyoki, Mod. Phys. Lett. B **7**, 397 (1993).
- [21] R. E. Blundell and A. J. Bray, Phys. Rev. A **46**, R6154 (1992).
- [22] M. Zapotocky, P.M. Goldbart and N. Goldenfeld, Phys. Rev. E **51**, 1216 (1995).
- [23] J.-i. Fukuda, Eur. Phys. J. B **1**, 173 (1998).
- [24] H. Furukawa, Adv. Phys. **34**, 703 (1985).
- [25] T. Ohta, D. Jasnow, and K. Kawasaki, Phys. Rev. Lett. **49**, 1223 (1982); K. Kawasaki, M. C. Yalabik, and J. D. Gunton, Phys. Rev. A **17**, 455 (1978).
- [26] G. F. Mazenko and R. A. Wickham, Phys. Rev. E **55**, 1321 (1997); R. A. Wickham and G. F. Mazenko, Phys. Rev. E **55**, 2300 (1997); G. F. Mazenko and R. A. Wickham, Phys. Rev. E **57**, 2539 (1998).
- [27] A. J. Bray and A. D. Rutenberg, Phys. Rev. E **49**, R27 (1994); A. D. Rutenberg and A. J. Bray, Phys. Rev. E **51**, 5499 (1995).
- [28] For multiple defect species, for instance with a $O(2) \times Z_2$ ground-state degeneracy [38] or for $d = 3$ nematic quenches [6], multiple length-scales may be common. It remains to be seen if these length-scales are coupled through the dynamics, i.e. if scaling violations occur.
- [29] A. Coniglio and M. Zannetti, Europhys. Lett. **10**, 575 (1989).
- [30] A. J. Bray and K. Humayun, Phys. Rev. Lett. **68**, 1559 (1992).
- [31] S. Ma and L. Senbetu, Phys. Rev. A **10**, 2401 (1974); L. Sasvári, F. Schwabl, and P. Szépfalusy, Physica **81A**, 108 (1975).
- [32] A. D. Rutenberg and A. J. Bray, Phys. Rev. Lett. **74**, 3836 (1995).
- [33] A. A. Ovchinnikov and Ya. B. Zeldovich, Chem. Phys. **28**, 215 (1978); D. Toussaint and F. Wilczek, J. Chem. Phys. **78**, 2642 (1983).
- [34] The analogy with an interacting particle system is not exact since vortices in the 2D XY model have effective mobilities that depend on the local structure (see discussion in [10]).
- [35] A. J. Bray and S. Puri, Phys. Rev. Lett. **67**, 2670 (1991); H. Toyoki, Phys. Rev. B **45**, 1965 (1992).
- [36] Existing correlation-closure schemes use the bare vortex configurations, while the logarithmic mobility and hence the logarithmic factor in the growth law comes from non-singular corrections to the tails of bare vortices [27]. This may be connected with the deviations between theory and simulation seen at large distances in Fig. 3, and also with the lack of logarithmic factors seen in correlation-closure schemes (R. Wickham, private communication).
- [37] A. D. Rutenberg and A. J. Bray, Phys. Rev. E **51**, R1641 (1995).
- [38] S. J. Lee, J.-R. Lee, and B. Kim, Phys. Rev. E **51** R1 (1995); J.-R. Lee, S. J. Lee, B. Kim, and I. Chang, Phys. Rev. E **54** 3257 (1996); *ibid* Phys. Rev. Lett. **79**, 2172 (1997); S. J. Lee, B. Kim, and J.-R. Lee, Phys. Rev. E **56**, 6362 (1997).
- [39] A. J. Bray, N. P. Rapapa, and S. J. Cornell, Phys. Rev. E **57**, 1370 (1998).
- [40] While the exponent of the leading correction to a growth law is probably universal (between, for example, $L_{1/2}$ and L_v), a non-universal shift in the amplitude ratio between the growth law and the leading correction is sufficient to shift the effective exponent at finite times.
- [41] M. Siegert, *Coarsening dynamics of crystalline thin films* (cond-mat/9808119).
- [42] Higher-point correlations that cannot be expressed in a simple scaling form [16] are subdominant, in that they only probe the vicinity of defects and thus have negligible weight compared to two-point correlations. It may be that multiple length-scales can be found in any system with singular defects if sufficiently high-order correlations, restricted to the vicinity of the defects, are considered.
- [43] One could argue that a scaling form for full two-time correlations, $C(r, t, t') \equiv \langle \vec{\phi}(x+r, t) \cdot \vec{\phi}(x, t') \rangle$, is the most natural since it would include autocorrelations. However this two-time correlation is impractical to measure and is not necessary to determine the scaling growth-law. We use a less restrictive definition of dynamical scaling, using only $C(r, t)$ and $T(r, t)$.
- [44] Conserved dynamics have also been explored in the 2D XY model, see M. Mondello and N. Goldenfeld, Phys. Rev. E **47**, 2384 (1993) and S. Puri, A. J. Bray, and F. Rojas, Phys. Rev. E **52**, 4699 (1995). No evidence of scaling violations is observed in these systems.
- [45] Liquid-crystal films can have significant and discernible differences from 2D XY systems (though see [3,5]). Most obvious are the non-abelian species of vortices seen in biaxial nematic films [22]. Less obvious is the different vortex structure, resulting from the “headless” nature of nematics [21] or from varying bend and twist elastic constants, which will change the Porod amplitude contributed by each vortex [M. Zapotocky and P. M. Goldbart, cond-mat/9812235]. While any *scaling* growth law must be the same in these systems, determined by the singular nature of the vortices [27] rather than their fine structure, it is possible that some planar systems with vortices do not dynamically scale.
- [46] A. J. Bray and K. Humayun, Phys. Rev. E **48**, 1609 (1992).
- [47] C. Yeung, Y. Oono, and A. Shinozaki, Phys. Rev. E **49**, 2693 (1994).
- [48] Y. Oono and S. Puri, Phys. Rev. Lett. **58**, 836 (1987); Phys. Rev. A **38**, 434 (1988); S. Puri and Y. Oono, *ibid* **38**, 1542 (1988).
- [49] N. Grønbech-Jensen, Int. J. Mod. Phys. C **7**, 873 (1996).
- [50] W. H. Press *et al*, *Numerical Recipes*, (Cambridge Univ. Press 1994).
- [51] P. M. Chaikin and T. C. Lubensky, *Principles of condensed matter physics* (Cambridge, UK, 1995).
- [52] E. M. Kramer, Phys. Rev. E **50**, 3594 (1994).

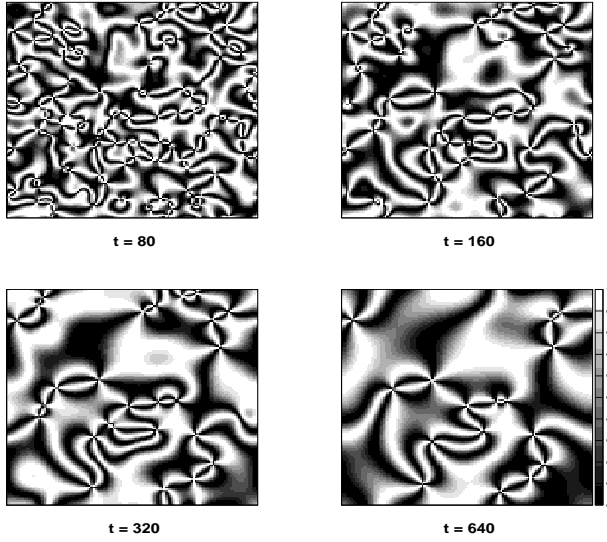


FIG. 1. Schlieren patterns in various times after a quench of the 2D XY model in a size 128×128 system. The intensity is $\sin^2(2\theta)$, where θ is the local XY phase. Each vortex emanates 8 brushes, alternating white and black.

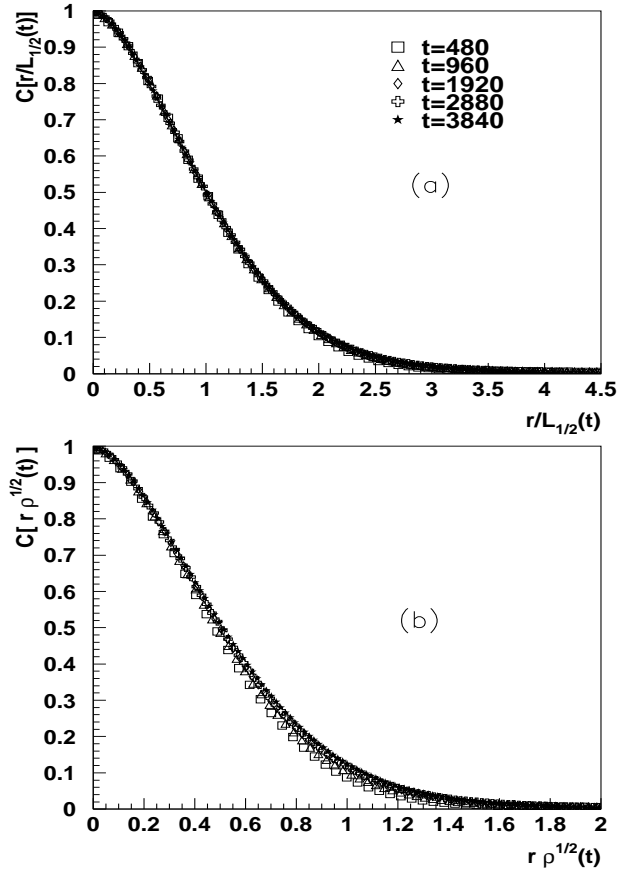


FIG. 2. a) Real-space correlations vs $x = r/L_{1/2}$, where $C(L_{1/2}) = 1/2$. The continuous curve represents the theoretical prediction, $f_{BPT}(x)$. b) Attempted scaling with respect to the vortex density.

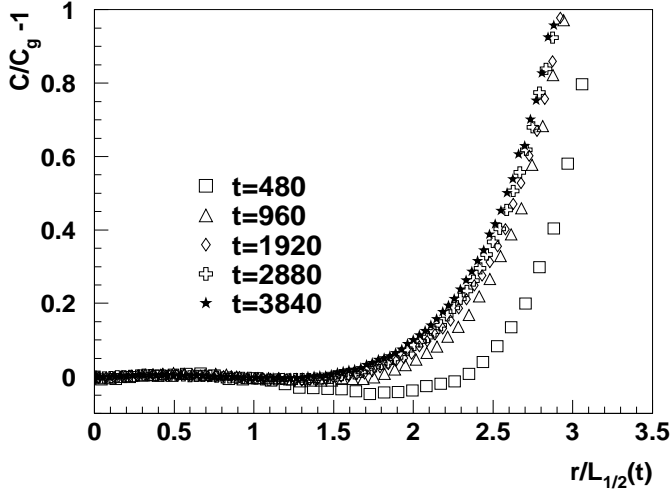


FIG. 3. The difference between measured correlations, $C(r,t)$, and the Gaussian-closure prediction, C_g , normalized by C_g and plotted against scaled distance.

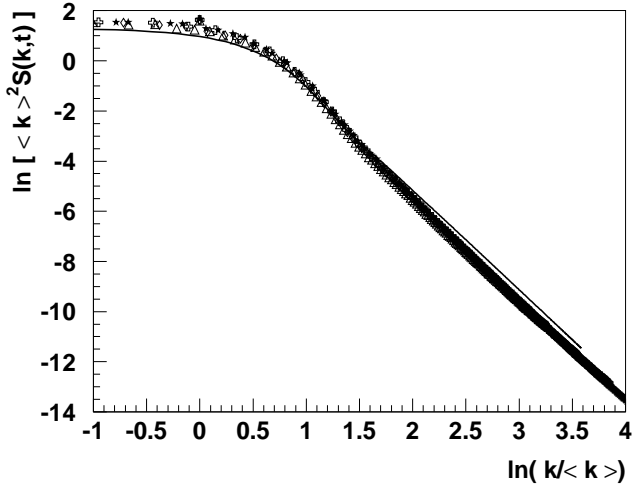


FIG. 4. The structure factor in a log-log Porod plot. The first moment, $\langle k \rangle$, is used to rescale momenta. The continuous line is the Gaussian-closure prediction. Symbols are the same as the previous figure.

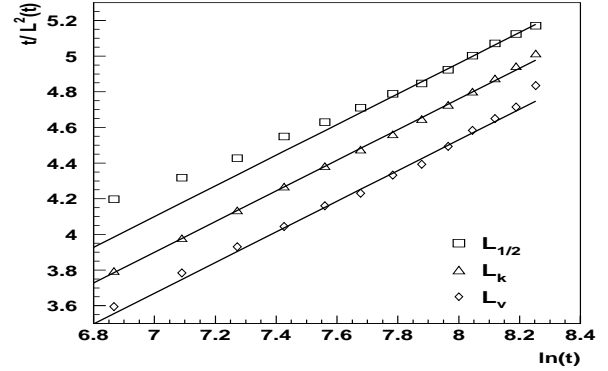


FIG. 5. We plot t/L^2 vs $\ln t$ for three lengths: $L_{1/2}$, L_k , and L_v . The observed linear dependence at late times indicates that the dynamical scaling growth law, Eqn. 2, holds. As shown by the parallel straight-lines, the offset (given by t_0) is non-universal.

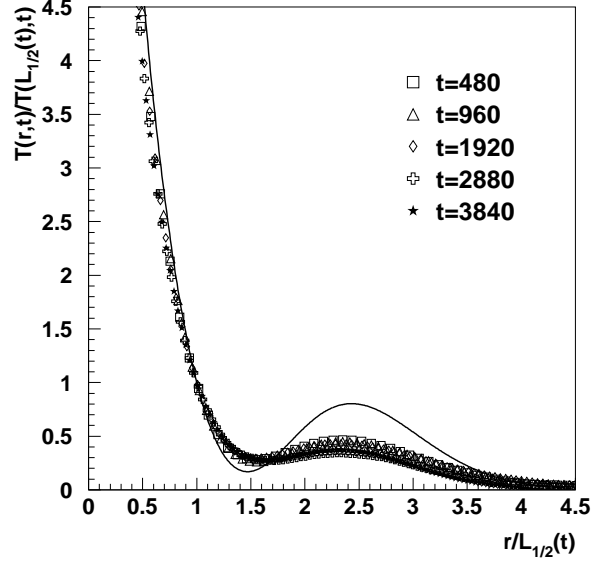


FIG. 6. Scaling plot of $T(r,t)/T(L_{1/2},t)$ vs $r/L_{1/2}$. The continuous curve is the theoretical prediction of the Gaussian closure scheme — significant deviations are apparent.

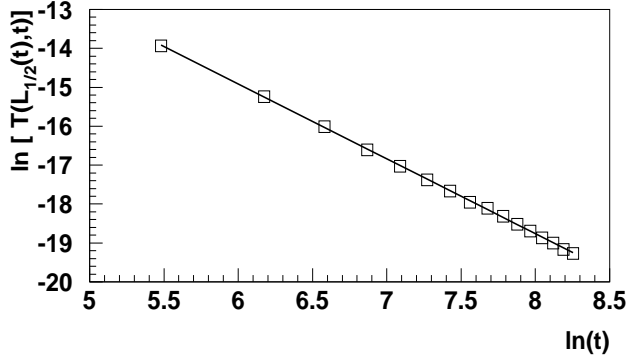


FIG. 7. Log-log plot of the time dependent prefactor of the time-derivative correlation function. The best fit over the range shown yields a decay $1/t^\mu$ with an exponent $\mu = 1.96$. Varying the fit range yields $\mu = 2.0 \pm 0.1$.

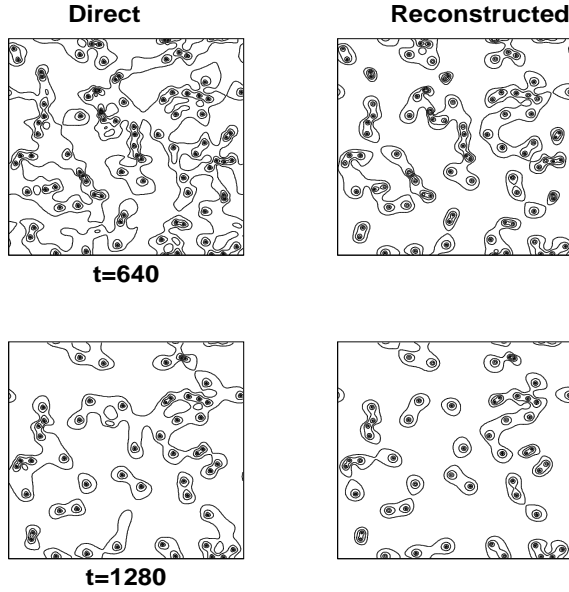


FIG. 8. Snapshots of $|\nabla\theta|$ for a 256×256 size system at two times after the quench. The left column shows the direct $|\nabla\theta|$, with contour levels at 0.1, 0.2, 0.4, 0.8, and 1.6. [Note that the lattice spacing defines a unit of length, so the largest gradient magnitude is π .] The right column shows $|\nabla\theta|$ periodically reconstructed using only the vortex positions, with the same contour levels. Significant differences between the direct and reconstructed $\nabla\theta$ field can be seen away from the immediate vicinity of the vortices.

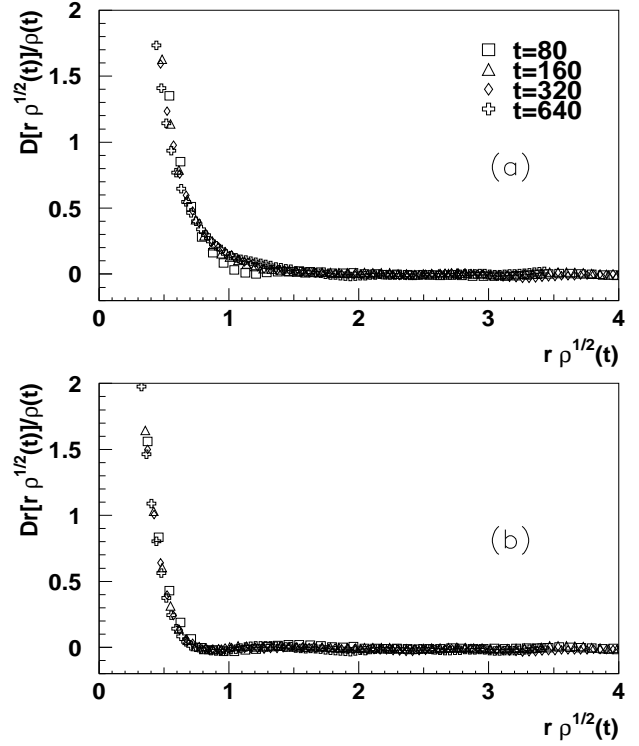


FIG. 9. Direct and reconstructed $\nabla\theta$ correlations, $D(r, t)$, and $D_r(r, t)$, respectively, normalized by vortex density for a scaling plot vs scaled distance. Scaling is observed after the earliest time.

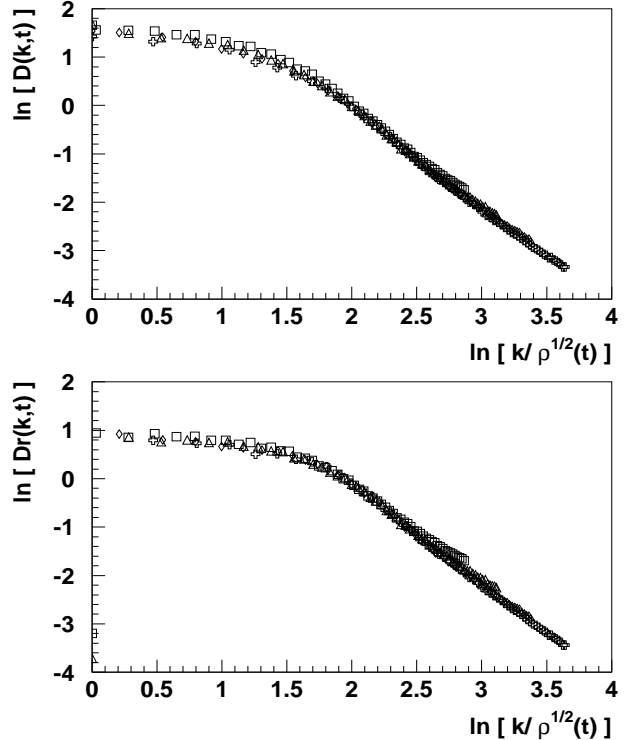


FIG. 10. Porod plots of Fourier-transformed direct and reconstructed $\nabla\theta$ correlations, $D(k, t)$ and $D_r(k, t)$, respectively. Symbols are the same as the previous figure.